From Cd-Rich to Se-Rich – The Manipulation of CdSe Nanocluster Structure and Optical Absorption

Marc Jäger*[a] and Rolf Schäfer[a]

A combined experimental and quantum-chemical study of the structure and optoelectronic properties of isolated non-stoichiometric $Cd_xSe_y^+$ clusters with x = 3, 4 and y = 3, 4 is presented. The consistency of optical response calculations with the measured absorption spectra reveals that the theoretically predicted lowest energy structural isomers have been formed in the molecular beam experiments. The Se-rich nanocluster $Cd_3Se_4^+$ contains a Se_2^- unit which is responsible for the enhanced light absorption in the visible spectral range. In contrast, the radical electron of the Cd-rich species $Cd_4Se_3^+$ is localized at a Cd^+ centre which is attached to a six-membered Cd_3Se_3 ring. The excess Cd atom is partly responsible for an intense optical absorption in the near ultraviolet. The variation of the geometry and the optical behaviour in dependence of the stoichiometry is discussed with respect to the photocatalytic properties of CdSe nanoparticles

Introduction

In the past decades, the exploration of smaller and smaller semiconductor materials has drawn significant attention in industry and fundamental research.[1–6] Especially so-called quantum dots (QDs)[7] consisting of II–VI semiconductor materials as CdSe exhibit intriguing optoelectronic properties, because its photoluminescence can be tuned by varying the particle size.[8] These characteristics highlight QDs as promising materials for optical applications such as light emitting diodes (LEDs), displays, biomedical imaging and lasers.[2,9–12] In most experimental studies, colloidal CdSe QDs were examined.[13–15] This means that the semiconductor nanoparticles (NPs) are surrounded by a chemical environment, i.e. the NPs are ligated and solvated. Especially the ligands have a strong influence on the optical properties, due to the saturation of dangling bonds at the surface of the QDs. In most cases, samples of colloidal QDs are poly-dispersed and, thus, show a size distribution which depends on the synthesis route. However, it is nowadays not only possible to synthesize and isolate colloidal QD samples with a well defined size[16–18] but also feasible to control the surface composition. By this, it was possible to study the influence of the surface stoichiometry on the optoelectronic and photocatalytic behaviour of CdSe NPs. The optical absorption shows for example a red-shift with increasing Se content.[19] It has been also found that a decrease in the surface Se ratio of CdSe QDs gives a more than 10-fold increase in solar H_2 evolution.[20] Additionally, a mechanistic study revealed that improving the Cd/Se stoichiometric ratio and exposing more active surface Cd atoms significantly enhances the activity of CdSe QDs for CO_2 photo-reduction.[21]

In order to get a fundamental understanding of how the optical behaviour of semiconductor nanoparticles changes with their size and chemical composition in detail, the investigation of isolated semiconductor species is necessary, because by this ligand and solvent effects are ruled out. Therefore, we have studied the influence of the stoichiometry on the geometric and electronic structure of isolated CdSe clusters, in order to peel out the intrinsic properties of the system. To work out the impact of stoichiometry, isolated clusters with an excess of Se or Cd are compared to the stoichiometric species. Comparing the experimentally measured absorption spectra with quantum-chemical calculations results in a detailed insight of the chemical bonding in CdSe nanoclusters. Single positively charged species have been investigated because the defect electron in the clusters acts as a sensitive probe for the electronic structure. To the best of our knowledge, there have been no experimental and theoretical studies of small, isolated, non-stoichiometric, cationic CdSe clusters yet.

Results and Discussion

The optical properties are experimentally probed by photodissociation spectroscopy. Structural candidates are obtained by global optimisation and predicted absorption spectra are derived by time-dependent density functional (TDDFT) calculations at the PBE0/cc-pVTZ-PP and B3LYP/cc-pVTZ-PP level of theory with the corresponding effective core potentials.[22–25] The experimental and computational methods are described in more detail in the methods section.

For the investigated non-stoichiometric species only one structural isomer in the energy range of 0.10 eV with respect to the predicted global minimum (GM) has been found. The geometric structures of the calculated GMs are depicted in Figure 1 together with the previously examined geometries of

[a] M. Jäger, Prof. Dr. R. Schäfer
Eduard-Zintl-Institut für Anorganische und Physikalische Chemie
Technical University of Darmstadt
Alarich-Weiss-Straße 8, 64287 Darmstadt, Germany
E-mail: jaeger@cluster.pc.chemie.tu-darmstadt.de

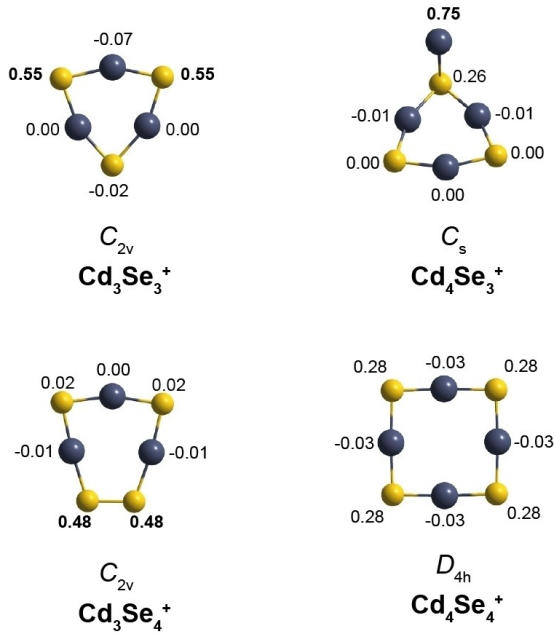

Figure 1. Lowest energy structures of $Cd_xSe_y^+$ clusters with $x = 3,\ 4$ and $y = 3,\ 4$ (Cd: dark atoms, Se: light atoms) obtained by global optimization. The point group symmetry as well as the relative electronic spin densities for each atom are shown. The largest values are highlighted with bold font.

$Cd_3Se_3^+$ and $Cd_4Se_4^+$.[26] Additionally, each atom is labelled by its relative electronic spin density. Similar to small stoichiometric species, the non-stoichiometric $Cd_xSe_y^+$ clusters prefer ring-like structures, for which the number of hetero-nuclear bonds is maximised. With with the exception of $Cd_4Se_3^+$, all atoms are two-fold coordinated. For stoichiometric CdSe clusters it is known that the hexagonal planar $Cd_3Se_3^+$ structure serves as a building block of larger CdSe NPs.[26–28] This geometry motif can also be found in $Cd_4Se_3^+$. Similar to the case of stoichiometric CdSe clusters, Cd favours a nearly linear coordination, whereas Se tends to form an angled configuration. All clusters examined here exhibit planar rings. The characteristic feature of the Se-rich cluster $Cd_3Se_4^+$ is the formation of a homoatomic Se–Se bond. In contrast, in the cluster with excess Cd, the additional Cd atom is attached to the six-membered $Cd_3Se_3^+$ ring, thereby forming one three-fold coordinated Se atom to preserve the ring-structure of $Cd_3Se_3^+$. The spin densities indicate that the defect electron in the $Cd_3Se_4^+$ is located on the Se_2 unit. In the stoichiometric species, the radical electron is also located almost exclusively on the Se atoms. If one considers that the chemical bond between Cd and Se has a strong ionic character, the $Cd_3Se_4^+$ cluster is built up from a $(Cd_3Se_2)^{2+}$ unit and a Se_2^- radical. In contrast, the spin densities of $Cd_4Se_3^+$ show a high value at the additional Cd atom, i.e. this cluster consists of a neutral Cd_3Se_3 unit and a Cd^+ radical. The questions to be addressed are whether these geometric structures can be observed in gas phase experiments and how the optical behaviour is influenced by the stoichiometry.

The experimental and TDDFT-computed optical response of the clusters are shown in Figure 2. For each cluster species, the

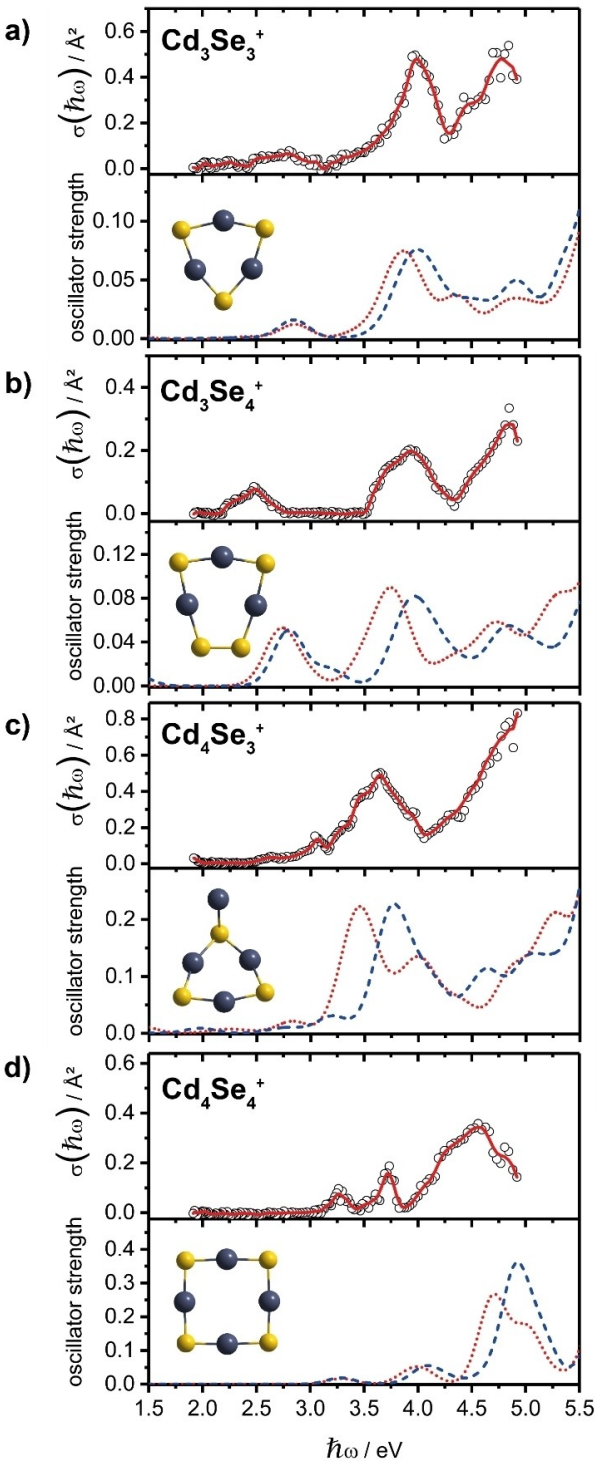

Figure 2. For each cluster: a) $Cd_3Se_3^+$, b) $Cd_3Se_4^+$, c) $Cd_4Se_3^+$, d) $Cd_4Se_4^+$, the experimental absorption cross section $\sigma(\hbar\omega)$ data points (black open circles) and a 5-pt adjacent average as a guide to the eye (solid redline) are compared to the optical absorption of the lowest-lying energy structures (Cd: dark atoms, Se: light atoms) computed with PBE0 (dashed blue line) and B3LYP (dotted red line) TDDFT calculations. The spectra are generated by Gaussian convolution of line spectra using a full width at half-maximum of 0.30 eV. The intensities of the spectra should not be considered quantitatively and serve to discriminate structures through qualitative comparison

experimental absorption spectrum (shown in the respective top-subfigure) is compared to optical response calculation for the predicted GM. In each experimental spectrum a 5-point adjacent average (solid red line) is added to emphasise the absorption trends. The results of the TDDFT calculations are line spectra which have been convoluted by Gaussians in order to facilitate a better comparison with experimental data. The outcomes of B3LYP calculation are depicted as dotted red lines and the PBE0 results are shown as dashed blue lines. Overall, for all chemical compositions, regardless of whether stoichiometric or non-stoichiometric species are considered, the experimental and simulated spectra match remarkably well. However, due to a low laser fluence and large fluctuations in the UV spectral region, the experimental data from 4.2 eV up to 5.0 eV are subjected to a larger error and could deviate with a higher probability (than absorption cross sections for lower energies) from the correct value. Analogously, the reliability of the TDDFT predictions decreases with higher electronic excitations as higher-lying orbitals are involved in the description. For instance, to reach 5.0 eV more than 50 electronically excited states have to be predicted for all clusters. Nevertheless, the good qualitative agreement between experiment and theory provides strong evidence that the predicted GM structures of the non-stoichiometric nanoclusters are actually formed in the molecular beam experiment. This also confirms that B3LYP/cc-pVTZ-PP as well as PBE0/cc-pVTZ-PP are well suited to describe the optical properties of $Cd_xSe_y^+$ clusters.[26,28] Absorption features of B3LYP calculations are more red-shifted in comparison to PBE0 results. It is striking that the absorption spectra strongly change with cluster composition and size. The addition of Cd or Se to the stoichiometric species leads to a shift of the absorption spectra to longer wavelengths, whereby the effect due to Se doping is much stronger pronounced. However, the Cd-rich cluster $Cd_4Se_3^+$ shows by far the strongest light absorption for wavelengths greater than 350 nm. This observation fits to investigations of CdSe NPs with an increased surface Cd ratio.[19]

The electronic structure analysis shows that the highest occupied valence molecular orbitals (MOs) for all species are almost exclusively made up of Se 4p basis functions. The lowest unoccupied MOs of $Cd_3Se_3^+$ and $Cd_3Se_4^+$ also consist exclusively of Se 4p basis functions, however, the species $Cd_4Se_3^+$ and $Cd_4Se_4^+$ additionally have a significant portion of Cd 5 s basis functions. It is known from bulk CdSe that its valence band is mainly built from Se 4p orbitals, while the conduction band is made up of Cd 4 s orbitals. The reason why Se 4p basis functions dominate the valence MOs of the cationic CdSe cluster species is caused by the positive net charge. As shown previously in a comparison between cationic $Cd_3Se_3^+$ and neutral Cd_3Se_3,[26] the molecular orbitals in the neutral species show an almost identical composition as the ones of the cation. Since the occupation of the MOs for neutral and cationic species is different, the LUMO of the cation resembles the HOMO of the neutral cluster, which is mainly built up of Se 4p basis functions in accordance to the electronic structure of bulk CdSe. According to this consideration, the LUMO + 1 of the cation corresponds to the LUMO of the neutral species and indeed the LUMO + 1 of all the cationic CdSe clusters shows a significant contribution of Cd 4 s basis functions for all species examined here. For a qualitative description of the chemical bonding, the natural localized molecular orbitals (NLMOS) are analysed. All clusters show Cd–Se bonds and the investigated Se-rich species also exhibits Se–Se bonds. The polar Cd–Se bonds are described by an overlap of sp hybrid orbitals of Cd with almost pure p orbitals of Se. The sp hybrid orbitals of Cd consist of roughly equal parts of Cd 5 s and Cd 5p basis functions, while the binding orbital of Se consists of more than 90% of Se 4p functions and less than 10% of Se 4 s functions. For the Se–Se unit in $Cd_3Se_4^+$ σ- and π-bonding occurs due to an overlap of orbitals which mainly are composed of Se 4p basis functions. For the stoichiometric species and the Se-rich cluster $Cd_3Se_4^+$, the electronic spin densities at the Cd centres are almost completely vanishing. The spin densities in the stoichiometric species are delocalized over the Se atoms. This is in contrast to the Se-rich cluster, in which the radical electron is exclusively located at the Se_2 unit thereby forming a superselenide Se_2^-. In the Cd-rich cluster $Cd_4Se_3^+$ the radical electron is mainly located at the excess Cd atom. Therefore, this cluster is best described as an atomic Cd^+ radical attached to a neutral Cd_3Se_3 unit.

The question now is how the different electronic structure of the Cd / Se-rich clusters affects their optical behaviour?

Therefore, we have analysed the dominant optical transitions for $Cd_4Se_3^+$ at around 3.5 eV and for $Cd_3Se_4^+$ at around 2.5 eV in terms of the natural transition orbitals (NTOs). The electronically excited states do not correspond to HOMO-LUMO transitions but involve several MOs near the HOMO-LUMO region. Furthermore, the transitions cannot be described in the one-electron approximation, i.e. a large number of molecular orbitals are involved in each case. Hence, if the electronic transitions are described based on NTOs, an electronic excitation consists of several (here, three for both transitions) NTO pairs. However, the NTO pair with the largest contribution ($\geq$50%) can be determined for each of the transitions to determine the character of the transition qualitatively. The corresponding iso-surfaces of the selected NTOs are shown in Figure 3. For the Se-rich cluster it becomes clear that only Se 4p orbitals are involved in the optical transition. Accordingly, for $Cd_3Se_4^+$ the low energy absorption can be characterized as a π–π* transition. It is interesting that for Se_2^- colour centres in the red selenium ultramarine also an intense π–π* transition at 2.5 eV is observed.[29] The electronic structure analysis results in a consistent picture for the Se-rich cluster: The Se_2 unit carries the radical electron and is largely responsible for the strongest light absorption in the visible spectral range in the experiment. In the Cd-rich cluster, on the other hand, there is an electron transfer from an initial state which is delocalized over the whole cluster to a Cd-dominated final NTO, with largest contribution at the excess Cd atom, on which also the radical electron is localized. Hence, in the framework of this NTO analysis the excess Cd atom is heavily involved in the electronic transition and thus, it is largely responsible for the particularly intense band at 3.5 eV .

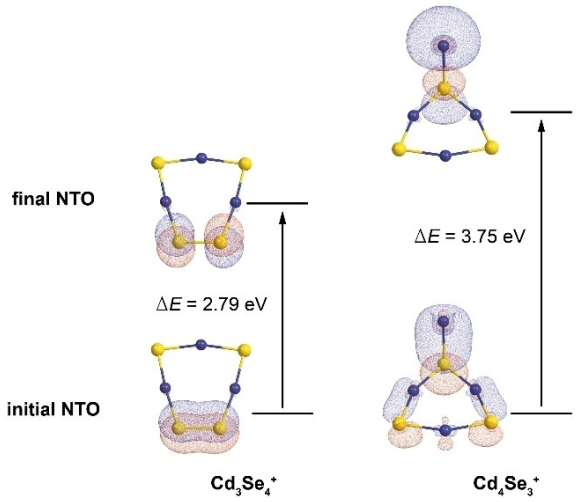

Figure 3. Dominant NTO pairs at the PBE0 level of theory for the low energy transition around 2.5 eV of $Cd_3Se_4^+$ and the huge optical absorption of $Cd_4Se_3^+$ around 3.5 eV. Iso-surfaces of the NTOs are shown and the exact PBE0 transition energies ΔE are given.

How do these results translate into the chemistry of Cd/Se-rich NPs? On the one hand, the absorption of light in the visible spectral range can be enhanced by an increased Se content, which should have a positive effect for photocatalytic applications using sunlight. The red shift in the optical absorption is less pronounced in the Cd-rich cluster. There are, however, particularly intense optical transitions in the near ultraviolet range. This strong light absorption is then responsible for an even more favourable photo-catalytic activity.

Conclusion

In this joint experimental and quantum-chemical study, the optical properties of isolated $Cd_xSe_y^+$ clusters with x = 3,4 and y = 3,4 are analysed. With the combined approach, the predicted geometric structures were confirmed. The Se-rich species $Cd_3Se_4^+$ contains a Se_2^- unit. The radical electron is localized at the Se_2 fragment and this part of the clusters is also responsible for the light absorption in the visible spectral range. In contrast, the Cd-rich cluster $Cd_4Se_3^+$ is formed by addition of an atomic Cd^+ radical to a neutral Cd_3Se_3 species, i.e. only heteronuclear bonds are formed. As part of the NTO analysis of the TDDFT results, the excess Cd leads to a significantly enhanced optical absorption in the near ultraviolet spectral range which might be favourable for an improved photo-catalytic performance of CdSe NPs with increasing Cd content. In order to be able to make more precise statements regarding the nature of the electronic transitions (e.g. occurrence of charge-transfer effects), multi-reference calculations are necessary which should be applied in future studies to the clusters examined here.

Methods Section

An in-depth presentation of the general methodology and experimental details are described elsewhere,[26,28] therefore, only a brief overview is given here. CdSe clusters are generated by a pulsed laser vaporization source and detected with time-of-flight mass spectrometry. Optical absorption spectra are recorded by photo-dissociation spectroscopy in the photon-energy range of $\hbar\omega = 1.9–4.9$ eV. All dissociation cross sections shown here can be regarded as lower limits to the absorption cross section, as discussed previously.[26]

Structural candidates of $Cd_xSe_y^+$ clusters with x = 3, 4 and y = 3, 4 are obtained by employing a genetic algorithm GA as described elsewhere.[26,28,30] All energetically lowest-lying isomers are locally re-optimised using NWChem v6.6[31] at the PBE0/cc-pVTZ-PP[22,24–25] and B3LYP/cc-pVTZ-PP[23–25] level of theory with the respective effective core potential (ECP). Hence, for Cd and Se, 20 and 24 electrons are treated explicitly, respectively. In a previous benchmark study, both exchange correlation (xc) functional/basis set combinations have pointed out to provide a very good description for $Cd_xSe_y^+$ clusters.[26,28] All lowest lying-energy structures exhibit a doublet electronic spin multiplicity i.e. quartet and sextet states are at least 0.8 eV higher in energy. Harmonic frequency analyses are performed for compositions at the particular level of theory in order to verify that the optimised geometries correspond to local minima on the potential energy surface. For the lowest energy candidates within a relative energy of 0.10 eV to the putative global minimum (GM), electronic excitation spectra are calculated using spin-unrestricted time-dependent density functional theory (TDDFT) with up to 120 excited states, employing the same xc functionals and basis sets including the ECPs as used during the geometry optimisation (GO). Furthermore, a natural bond analysis (NBA) was performed to calculate relative electronic spin densities and natural localised molecular orbitals (NLMOs) for deeper insights into the chemical bonding.

Acknowledgements

We thank Andreas Lehr and Vera Krewald for helpful discussions and we acknowledge financial support from the Deutsche Forschungsgemeinschaft (grant SCHA 885/15-2) and COST action MP0903 (NANOALLOYS). M. Jäger acknowledges a scholarship of the Merck'sche Gesellschaft für Kunst und Wissenschaft. Open access funding enabled and organized by Projekt DEAL.

Conflict of Interest

The authors declare no conflict of interest.

Keywords: CdSe · Semiconductor · Cluster · Optical Absorption · Atomically-Precise Nanoclusters

[1] M. M. Waldrop, *Nature* **2016**, *530*, 144–147.
[2] Y. Shirasaki, G. J. Supran, M. G. Bawendi, V. Bulović, *Nat. Photonics* **2013**, *7*, 13–23.
[3] M. K. Choi, J. Yang, T. Hyeon, D.-H. Kim, *npj Flex. Electron.* **2018**, *2*, 10.
[4] A. P. Alivisatos, *Science* **1996**, *271*, 933–937.
[5] P. Yang, R. Yan, M. Fardy, *Nano Lett.* **2010**, *10*, 1529–1536.

[6] S. Gupta, W. T. Navaraj, L. Lorenzelli, R. Dahiya, *npj Flex. Electron.* **2018**, *8*, 1–18.
[7] S. Reimann, M. Manninen, *Rev. Mod. Phys.* **2002**, *74*, 1283–1342.
[8] L. Liu, Q. Peng, Y. Li, *Inorg. Chem.* **2008**, *47*, 5022–5028.
[9] Y. E. Panfil, M. Oded, U. Banin, *Angew. Chem. Int. Ed.* **2018**, *57*, 4274–4295.
[10] D. Bera, L. Qian, T. K. Tseng, P. H. Holloway, *Materials* **2010**, *3*, 2260–2345.
[11] J. M. Klostranec, W. C. W. Chan, *Adv. Mater.* **2006**, *18*, 1953–1964.
[12] J. M. Pietryga, Y. S. Park, J. Lim, A. F. Fidler, W. K. Bae, S. Brovelli, V. I. Klimov, *Chem. Rev.* **2016**, *116*, 10513–10622.
[13] C. B. Murray, D. J. Norris, M. G. Bawendi, *J. Am. Chem. Soc.* **1993**, *115*, 8706–8715.
[14] C. D. M. Donegá, R. Koole, *J. Phys. Chem. C* **2009**, *113*, 6511–6520.
[15] C. Leatherdale, W. Woo, *J. Phys. Chem. B* **2002**, *106*, 7619–7622.
[16] Y. Zhou, R. Jiang, Y. Wang, H. W. Rohrs, N. P. Rath, W. E. Buhro, *Inorg. Chem.* **2019**, *58*, 1815–1825.
[17] Y. Wang, Y. Zhang, F. Wang, D. E. Giblin, J. Hoy, H. W. Rohrs, R. A. Loomis, W. E. Buhro, *Chem. Mater.* **2014**, *26*, 2233–2243.
[18] Y. Wang, Y. H. Liu, Y. Zhang, F. Wang, P. J. Kowalski, H. W. Rohrs, R. A. Loomis, M. L. Gross, W. E. Buhro, *Angew. Chem. Int. Ed.* **2012**, *51*, 6154–6157.
[19] J. Jasieniak, P. Mulvaney, *J. Am. Chem. Soc.* **2007**, *129*, 2841–2848.
[20] M. Y. Huang, X. B. Li, Y. J. Gao, J. Li, H. L. Wu, L. P. Zhang, C. H. Tung, L. Z. Wu, *J. Mater. Chem. A* **2018**, *6*, 6015–6021.
[21] W. Xia, J. Wu, J. C. Hu, S. Sun, M. De Li, H. Liu, M. Lan, F. Wang, *ChemSusChem* **2019**, *12*, 4617–4622.
[22] C. Adamo, V. Barone, *J. Chem. Phys.* **1999**, *110*, 6158–6170.
[23] A. D. Becke, *J. Chem. Phys.* **1993**, *98*, 5648–5652.
[24] D. Figgen, G. Rauhut, M. Dolg, H. Stoll, *Chem. Phys.* **2005**, *311*, 227–244.
[25] K. A. Peterson, C. Puzzarini, *Theor. Chem. Acc.* **2005**, *114*, 283–296.
[26] M. Jäger, J. Schneider, R. Schäfer, *J. Phys. Chem. A* **2019**, *124*, 185–196.
[27] E. Sanville, A. Burnin, J. J. BelBruno, *J. Phys. Chem. A* **2006**, *110*, 2378–2386.
[28] M. Jäger, A. Shayeghi, V. Klippenstein, R. L. Johnston, R. Schäfer, *J. Chem. Phys.* **2018**, *149*, 244308–1-244308–14.
[29] H. Schlaich, G. G. Lindner, J. Feldmann, E. O. Göbel, D. Reinen, *Inorg. Chem.* **2000**, *39*, 2740–2746.
[30] M. Jäger, R. Schäfer, R. L. Johnston, *Nanoscale* **2019**, *11*, 9042–9052.
[31] M. Valiev, E. J. Bylaska, N. Govind, K. Kowalski, T. P. Straatsma, H. J. J. Van Dam, D. Wang, J. Nieplocha, E. Apra, T. L. Windus, W. A. de Jong, *Comput. Phys. Commun.* **2010**, *181*, 1477–1489.

Manuscript received: October 27, 2020
Accepted manuscript online: December 4, 2020
Version of record online: December 23, 2020